

Anatase Nanoparticles for Raman Nanothermometry

Thomas Pretto¹, Marina Franca¹, Veronica Zani^{1,2}, Silvia Gross¹, Danilo Pedron^{1,2}, Roberto Pilot^{1,2},
Raffaella Signorini^{1,2}

¹Department of Chemical Science
Via Marzolo 1, I-35123 Padova, Italy

thomas.pretto@studenti.unipd.it, marina.franca@phd.unipd.it, veronica.zani@phd.unipd.it,
silvia.gross@unipd.it, daniло.pedron@unipd.it, roberto.pilot@unipd.it, raffaella.signorini@unipd.it

²Consorzio INSTM,
Via G. Giusti 9, I-50121 Firenze, Italy

Abstract - The determination of the local temperature is an interesting and intriguing topic in the nanotechnology and nanomedicine world, in terms of tuning the best noninvasive measurement protocol and identification of the more versatile and performing material. In this paper, the Raman technique and titania NPs have been exploited for the realization of a new optical nanothermometer. Biocompatible titania NPs have been properly synthesized, following a combination of sol-gel and solvothermal green synthesis approaches, with the aim of obtaining samples of pure anatase, characterized by crystallite dimensions defined and good control over the final morphology and dispersibility. Powder XRD measurements and room temperature Raman measurements confirmed that the synthesized samples are single-phase anatase. The SEM images clearly showed the nanometric dimension of NPs. Stokes and anti-Stokes Raman measurements, collected with the excitation laser at 514.5 nm (CW Ar/Kr ion laser), substantiate the possibility of evaluating the local temperature, which has been tested in the range of 298 - 313 K, a range of interest for biological applications. The power of the laser has been carefully chosen in order to avoid eventual heating due to the laser irradiation. The data show that TiO₂ NPs possess a high sensitivity and low uncertainty in the range of a few degrees as Raman nanothermometer material.

Keywords: Temperature, Nanothermometer, Raman, Non-contact technique, Anatase, Nanoparticles, Green synthesis

1. Introduction

Temperature (T) is considered one of the most fundamental parameters: temperature sensors are widely used in daily life and are expected to reach a market of \$6 billion by 2023 [1]. The development of nanotechnology and nanomedicine [2,3] has brought about the need to monitor temperature on the nanoscale in contactless mode (nanothermometry) and therefore has stimulated the development of new methodologies, tools, and materials to achieve this goal, with the final focus of attaining high temperature sensitivity, minimum thermal uncertainty, and higher spatial resolution.

In this field, Raman spectroscopy is emerging as an interesting optical noncontact tool for temperature measurements [4]. Its main advantages include the ease of sample preparation, the wide range of detectable temperatures, and the large availability of materials that possess a Raman spectrum [5]. Moreover, it is characterized by a high spatial resolution, in the order of the diffraction limit of the laser probe [6].

Titanium dioxide perfectly fits all the requirements for a good thermometer material; it possesses a large Raman diffusion cross section, a high-intensity peak at low values of Raman shift, which is well defined and distinguishable from others, and it has low absorbance in a wide wavelength range. Moreover, it has also interesting chemical characteristics, such as high chemical stability and non-toxicity. Furthermore, commercial TiO₂ NPs have already been shown to have a good property as Raman active nanothermometers in the visible range [7,8].

In the literature, numerous sol-gel syntheses of titania have been reported, however they often require a calcination step, at temperatures above 500°C. Some articles report sol-gel methods combined with the use of ultrasound treatments [9], or the use of reflux conditions with at 70°C [10], while others adopt and solvo/hydrothermal treatments, taking advantage of mild reaction conditions [11], to control the size and shape of nanoparticles. Sol-gel and solvothermal syntheses allow control of the shape, size, structure, and composition control of NPs by tailoring parameters, such as temperature, reaction time, amount, and ratio of reactants, additives, and ligands.

In this work, titanium dioxide, as anatase polymorph, NPs have been properly synthesized following a combination of sol-gel and solvothermal synthetic approaches, to obtain samples of pure anatase, with defined crystallite dimensions. The synthesis process of anatase nanoparticles has been optimized and fine-tuned, in compliance with sustainability criteria from a green perspective. TiO₂ NPs have been characterized by SEM, XRD and Raman techniques. In particular, their nanothermometer properties have been evaluated in the visible region, at 514.5 nm, by anti-Stokes and Stokes Raman measurements collected in the 298 - 313 K range.

2. Materials and Methods

Titanium [IV] tetra-isopropoxide (Ti(OiPr)₄, 97% by weight in isopropanol, Merck 546-68-9), was dissolved in water and ethylene glycol (99% pure, Carlo Erba) and tetraethylammonium hydroxide (TEAOH, 35% by weight in water, Sigma-Aldrich), using the following optimized molar ratios: mol(H₂O)/mol(Ti(OiPr)₄)=150 and mol(TEAOH)/mol(Ti(OiPr)₄)=4.5. After 30-40 minutes of magnetic stirring, at room temperature, the solution is transferred to a Parr stainless steel hydrothermal bomb (Model 4745 General Purpose Acid Digestion Vessel, 23 mL volume, limit temperature of use 150°C, held up to 483 bar), which is then heated at 150°C for 24 h. The synthesis leads to the formation of a white precipitate which is isolated by centrifugation and washed with deionized water and ethanol. To obtain a nanocrystalline powder, the precipitate was dried in a silica gel dryer and placed under vacuum for one night.

SEM was performed with a Zeiss Sigma HD microscope, equipped with a Schottky FEG source, one detector for backscattered electrons and two detectors for secondary electrons (InLens and Everhart Thornley). The topographic measurements were performed at 20 kV. X-ray diffractometry (XRD) was used to analyse the crystal structure and crystallite size NPs. The diffractograms of the samples were acquired with a Bruker D8 Advance diffractometer, using a CuK α ($\lambda = 1.5406 \text{ \AA}$) radiation source. The range was $2\theta = 20^\circ\text{-}80^\circ$, with a scan step of $0.026^\circ 2\theta$, and 0.3 s acquisition per step. The crystallographic phase identification was performed using a Search & Match procedure, using Bruker Diffrac EVA software.

Two Raman setups were used to collect Raman spectra: 1) Micro-Raman equipped with an Ar⁺ laser @ 514.5 nm (Spectra Physics, Stabilite 2017), output power 1W. The back-scattered Raman signal, separated from the Rayleigh scattering by an edge filter, was analysed with a 320 mm focal length imaging spectrograph and a liquid nitrogen cooled CCD camera. 2) Micro-Raman setup equipped with an Ar⁺/Kr⁺ gas laser (Coherent, Innova 70), providing the line at 514.5 nm. The laser beam was coupled to a microscope (Olympus BX 40) and focused on the sample by 100x, 50x, or 20x objectives (Olympus SLMPL). Raman scattering was coupled into the slit of a three-stage subtractive spectrograph made up of a double monochromator (Jobin Yvon, DHR 320), working as a tunable filter rejecting elastic scattering, and a spectrograph (Jobin Yvon, HR 640). The Raman signal was detected by a liquid nitrogen cooled CCD. The Raman instruments were interfaced with a temperature control stage (Linkam, THMS600/720), used to control the sample temperature, in the range of 77-600 K. The sample was uniformly heated/cooled to reach the desired temperature, with a rate of 2 K/minute and a thermalization time of at least 15 minutes. Once the thermalization process was done, consecutive Stokes and anti-Stokes measurements were conducted, repeated to obtain a consistent set of data, to calculate the local temperature of the sample. Usually, for temperature measurements, a power intensity of 1 mW was used to avoid laser-induced heating.

3. Results and Discussion

The morphology of NPs is observable from SEM image, reported in Figure 1.1: ellipsoidal NPs with dimensions in the range 140-350 nm are clearly evidenced. The X-ray diffraction pattern of the sample, reported in Figure 1.2, demonstrates the crystalline nature of the anatase phase. From the Lorentzian deconvolution of the (101) peak (Red line of Figure 1.2), through the Scherrer equation, an effective crystalline size $D_{\text{eff}}=42 \text{ nm}$ has been evaluated. The Stokes Raman spectra, recorded at room temperature, using a laser at 514.5 nm, with an input power of 1 mW, have been acquired in 10 different positions of the sample.

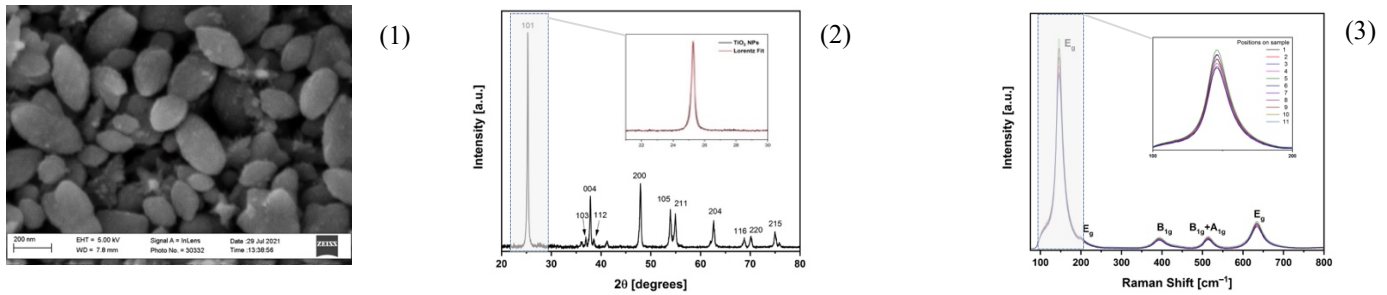


Fig. 1: SEM image (1), XRD pattern, with zoom in on 101 peak (2), and Raman spectra collected at 514.5 nm, at room T, in different positions of TiO₂ NPs, with zoom in on mode E_g (3).

The spectra, reported in figure 1 (3), clearly show an intense peak centred at 145.5 cm⁻¹ and four peaks at 199, 392, 514 and 634 cm⁻¹ with lower intensity. These signals, characteristic of the anatase phase, possess a high and uniform intensity in all regions of the sample.

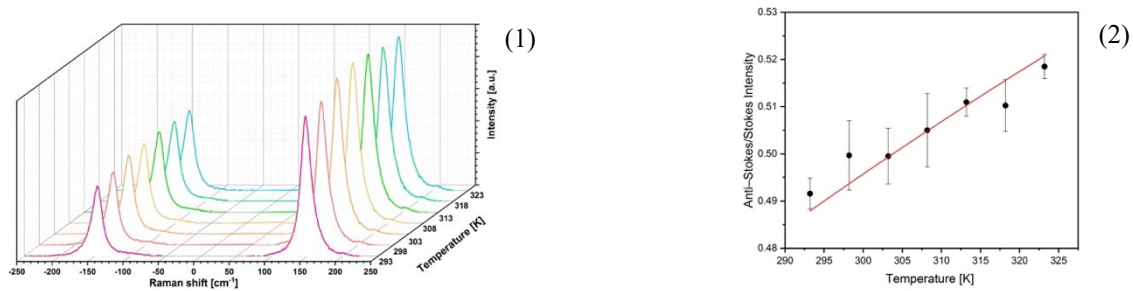


Fig. 2: Stokes and anti-Stokes spectra of the 145.5 cm⁻¹ E_g mode, as a function of temperature, from 283 to 323 K, with a step of increase of 5 K (1) and anti-Stokes/Stokes intensity ratios of the 145.5 cm⁻¹ E_g anatase mode (black dots) as a function of temperature, with the corresponding fitting curve, red line (2).

Table 1: Stokes and anti-Stokes intensities of the TiO₂ E_g peak and anti-Stokes/Stokes ratios for the temperature range 283 to 323 K.

T [K]	Anti-Stokes Intensity	Stokes Intensity	Anti-Stokes/Stokes Ratio
293	1797	3655	0.492±0.003
298	1881	3765	0.500±0.007
303	2038	4080	0.500±0.006
308	2102	4163	0.505±0.008
313	2098	4105	0.511±0.003
318	2076	4069	0.510±0.006
323	2087	4025	0.519±0.003

The anti-Stokes and Stokes Raman spectra of anatase have been collected in the temperature range of 283-323 K, by excitation at 514.5 nm, using an input power of 1 mW, and are reported in Figure 2.1.

All anti-Stokes and Stokes Raman spectra have been analysed with Matlab, using a Lorentz fitting, to obtain the Raman spectrum parameters, such as the intensity of the peak, reported in Table 1. The determination of intensity allows to determine the anti-Stokes/Stokes intensity ratio, also reported in Table 1 and Figure 2.2, which is the experimental parameter proportional to the temperature [12]. From the linear fitting of ratios, the experimental constant of 0.942±0.002 has been

found; the determination of this constant is a key point to correlate the Raman signal to the temperature. This value agrees with the value obtained, at the same excitation wavelength, with commercial TiO₂ NPs [7], where a high sensitivity and an uncertainty of few degrees have been demonstrated and confirms the possibility of using Anatase NPs as a nanothermometer.

4. Conclusion

The outcome of the Raman measurements on titanium dioxide NPs, properly synthesized following the combination of sol-gel and solvothermal synthesis approaches is very encouraging. It substantiates the possibility of evaluating the local temperature, in the biological range of 298 - 313 K, in the visible region. Data confirm that TiO₂ NPs are good Raman nanothermometers, possessing high sensitivity and low uncertainty in the range of few degrees, they allow the measurement of the local temperature, through Raman technique.

Acknowledgements

This research was funded by the Department of Chemical Science of the University of Padova, project P-DiSC#10BIRD2019-UNIPD.

References

- [1] C.D.S. Brites, S. Balabhadra and L.D. Carlos, "Lanthanide-Based Thermometers: At the Cutting-Edge of Luminescence Thermometry", *Adv. Optical Mat.*, 7, 1801239, 2019.
- [2] D. Jaque and F. Vetrone, "Luminescence nanothermometry", *Nanoscale*, 4, 4301-4326, 2012.
- [3] C.D.S. Brites, P. P. Lima, N.J.O. Silva, A. Millán, V.S. Amaral, F. Palacio, L.D. Carlos, "Thermometry at the nanoscale" *Nanoscale* 4(16), 4799-4829, 2012.
- [4] M. Quintanilla and L.M. Liz-Marzan, "Guiding Rules for Selecting a Nanothermometer," *Nano Today*, 19, 126–145, 2018.
- [5] R.L. McCreery, *Raman Spectroscopy for Chemical Analysis*; Wiley -Interscience, John Wiley and Sons, Ed. J.D.Winefordner, Hoboken, NJ, USA, 2000.
- [6] J.R. Serrano, L.M. Phinney, S.P. Kearney, "Micro-Raman Evaluation of Polycrystalline Silicon MEMS Devices," *Surf. Eng. Manuf. Appl.* 2006, doi:10.1557/PROC-0890-Y08-37.
- [7] V. Zani, D. Pedron, R. Pilot, R. Signorini, "Contactless Temperature Sensing at the Microscale Based on Titanium Dioxide Raman Thermometry," *Biosensors*, 11,102, 2021.
- [8] J. J. Gallardo, J.Navas, D. Zorrilla, R.Alcantara, D. Valor, C. Fernandez-Lorenzo, J. Martín-Calleja. "Micro-Raman Spectroscopy for the Determination of Local Temperature Increases in TiO₂ Thin Films due to the Effect of Radiation," *Applied Spectroscopy*, 1–9, 2015.
- [9] H.U. Lee, S.C. Lee, J.H. Seo, W.G. Hong, H. Kim, H.J. Yun, H.J Kim, J. Lee, "Room temperature synthesis of nanoporous anatase and anatase/brookite TiO₂ photocatalysts with high photocatalytic performance," *Chem. Eng. J.*, 223, 209 21, 2013.
- [10] A. Antonello, G. Brusatin, M. Guglielmi, V. Bello, G. Mattei, G Zacco, A. Martucci, "Nanocomposites of titania and hybrid matrix with high refractive index", *J. Nanopart. Res.*, 13, 1697-1708, 2011.
- [11] N. Uekawa, N. Endo, K. Ishii, T.Kojima, K.Kakegawa, "Characterization of Titanium Oxide Nanoparticles Obtained by Hydrolysis Reaction of Ethylene Glycol Solution of Alkoxide," *J. of Nanotechnology*, 102361-8, 2012.
- [12] B.J Kip, R.J. Meier, "Determination of the Local Temperature at a Sample during Raman Experiments Using Stokes and Anti-Stokes Raman Bands," *Appl. Spectrosc.*, 44, 707–711, 1990.